BOLETIN DE LA SOCIEDAD ESPAÑOLA DE
Cerámica y Vidrio
www.elsevier.es/bsecv

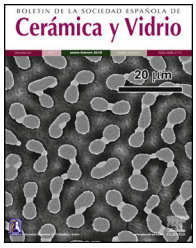

Mineralogical analysis of Brazilian Portland cements by the Rietveld method with emphasis on polymorphs M1 and M3 of alite

Cleusa M. Rossetto[a], *Geraldo L. Carezzatto*[b], *Luis G. Martinez*[b], *Marcelo Pecchio*[c], *Xavier Turrillas*[d,e,*]

[a] *Faculdade de Tecnologia de São Paulo – Fatec-SP, Depto de Edifícios, Praça Coronel Fernando Prestes, 30, Bloco A, Térreo, Bom Retiro, 01124-060 São Paulo, Brazil*
[b] *Centro de Ciência e Tecnologia de Materiais, Instituto de Pesquisas Energéticas e Nucleares, Av. Prof. Lineu Prestes 2242, São Paulo, SP 05508-000, Brazil*
[c] *Associação Brasileira de Cimento Portland – ABCP, Av. Torres de Oliveira, 76 – Jaguaré, São Paulo, SP 05347-902, Brazil*
[d] *Department of Advanced Crystallography, Institut de Ciència de Materials de Barcelona, ICMAB-CSIC, UAB Campus, E-08193 Cerdanyola del Vallès, Barcelona, Spain*
[e] *Experiments Division, ALBA Synchrotron Light Source, Carrer de la Llum, 2-26, E-08290 Cerdanyola del Vallès, Barcelona, Spain*

ARTICLE INFO

Article history:
Received 13 June 2022
Accepted 17 June 2022
Available online 7 July 2022

Keywords:
Mineralogical analysis
Synchrotron X-ray diffraction
Portland cement
Portland clinker
Alite polymorphs
Rietveld analysis

ABSTRACT

Eight samples of Portland cement and a clinker provided by the Brazilian Association of Portland Cement were analysed with different laboratory diffractometers and a synchrotron instrument to determine the statistical variability in the determination of the mass percentage of the main crystalline phases. Five laboratories participated in the experiment. Data collection was performed by each laboratory following its own internal procedures for a standard Rietveld analysis of mineral phases. Both Cu and Mo radiations were used. Reflection geometries—with and without sample rotation—and transmission geometries were also used. The synchrotron diffraction pattern was acquired from a rotating capillary and a wavelength of 0.41290 Å. Analysis of all diffraction patterns was performed with the help of TOPAS Academic v. 6 with the specific purpose of determining the proportions of polymorphs M1 and M3 of alite, since their ratio must be taken into account for the subsequent development of the mechanical properties of concrete.

Análisis mineralógico de cementos Portland de Brasil por el método de Rietveld con énfasis en los polimorfos M1 y M3 de la alita

Palabras clave:
Análisis mineralógico
Difracción con radiación sincrotrón
Cemento Portland

RESUMEN

Se analizaron ocho muestras de cemento y clínker Portland proporcionados por la Asociación Brasileña de Cemento Portland con diferentes difractómetros de laboratorio y una instalación de sincrotrón para determinar la variabilidad estadística de la determinación del porcentaje de masa de las principales fases cristalinas. Cinco laboratorios participaron

* *Corresponding author.*
E-mail address: xturrillas@icmab.cat (X. Turrillas).
https://doi.org/10.1016/j.bsecv.2022.06.005

Clínquer de Portland
Polimorfos de Alita
Análisis de Rietveld

en el experimento. La recopilación de datos fue realizada por cada laboratorio siguiendo sus procedimientos internos para un análisis estándar de Rietveld de fases minerales. Se utilizaron radiaciones de Cu y Mo. También se utilizaron geometrías de reflexión, con y sin rotación de la muestra, y de transmisión. El difractograma de sincrotrón se adquirió a partir de un capilar giratorio con una longitud de onda de 0,41290 Å. El análisis de todos los difractogramas se realizó con la ayuda de TOPAS Academic v. 6 con el propósito específico de determinar las proporciones de los polimorfos de alita M1 y M3, ya que su relación ha detenerse en cuenta en el desarrollo posterior de las propiedades mecánicas del hormigón.

Introduction

The determination of crystalline phases in cementitious materials by diffraction and subsequent Rietveld analysis [1] is a mature technique and the studies establishing the basis for its implementation are firmly established. The historical sequence of progress in the mineralogical analysis of Portland cementitious materials can be traced through the publications enumerated in chronological order in the following paragraph. The work of Scarlett and Madsen [2] dealt with in situ monitoring of phase abundances in the cement kiln. Another contribution of Pritula and Smrcok [3] was focused on the determination of mineral phases in NIST reference clinkers. A first Round Robin exercise was reported by Stutzman [4] and several laboratories participated to determine the mineral composition of synthetic cements prepared from mixtures of NIST SRM clinkers with controlled amounts of additional cementitious phases. A few years later another round robin test was published by León-Reina et al. [5]. In this work the analyses of two sets—both artificial and commercial— were reported. Another contribution to the subject was the work of Aranda et al. [6] which included also the quantitative analysis of the Portland hydration products. The round robin analysis published by Stutzman [7] involved 29 laboratories to evaluate two specimens of Portland cement with the aim of assessing precision and accuracy. Another interesting work that collects everything related to the diffraction of powders in Portland-type cements up to that moment is the chapter by Snell [8]. Gualtieri et al. [9] published a brief article that succinctly covered the most relevant aspects to take into account when performing mineralogical analyses using the Rietveld method. Finally Aranda et al. in a whole chapter of the International Tables for Crystallography [10] systematically collect all the knowledge on the mineralogical analysis of cements by means of powder diffraction techniques. This brief compilation of works would not be complete without citing a final contribution from Rowles [11], in which, after analysing round robin data published two decades ago, he presents some interesting conclusions with advice on how to correctly carry out mineralogical analyses using the Rietveld method.

The fore mentioned publications paved the way for the implementation of a norm to regularise the quality control of Portland cementitious materials. Their studies summarise with some detail the procedures and good practices to be followed spanning from the preparation of specimens to the strategies of diffraction data collection and encompassing the exercise of Rietveld analysis itself.

In order to rigorously apply the quantitative Rietveld analysis further efforts were invested to establish the crystal structures of the various polymorphs of the major phase of Portland cement, tricalcium silicate, also known as alite. This compound exhibits a number of polymorphs with temperature transitions well established. Schematically and according to Taylor [12] the seven high temperature phases can be represented by the sequence:

T1	T2	T3	M1	M2	M3	R
T °C	620 °C	920 °C	980 °C	990 °C	1070 °C	1080 °C

There are three triclinic phases, three monoclinic ones and finally another rhombohedral stable above 1070 °C. M1 and M3 are the most stable polymorphs of alite and sometimes the triclinic polymorph T2 can be present at room temperature, most likely due to a slow cooling. M1 is favoured by the presence of sulphur, and M3 by the presence of periclase and alumina, and small amounts of Fe_2O_3, Al_2O_3, MgO [13]. Higher proportions of SO_3 stabilise high temperature crystalline structures that can appear at room temperature, see Ludwig and Zhang [14]. De la Torre et al. [15] also did a comprehensive study of the influence of magnesium presence on the crystal structure of various polymorphs of alite. Experiments of high resolution with synchrotron radiation [16] allowed to determine the presence of the various polymorphs of alite. An extension of these studies to clarify the complex subject of alite polymorphs was endeavoured in the publication of De la Torre et al. [17] dealing with their crystal structure determination using a combined approach of diffraction data acquired by both neutron and synchrotron sources. Equally the work of Dunstetter et al. [18] and De Noirfontaine et al. [19] did throw light into this subject.

In the last few years it has been recognised that the relative ratio between the polymorphs M1 and M3 of alite has influence on the subsequent development of mechanical properties [20]. Despite knowledge in some detail of the crystal structures of the M1 and M3 polymorphs, in practice it is not easy to discriminate and quantify exclusively by Rietveld analysis both. Usually the Rietveld analysis is accomplished by defining an “average” superstructure of alite and therefore it is determined as a single phase. For many purposes that may be sufficient, but if that is not the case another approach has to be enforced. The software for Rietveld Analysis, Academic TOPAS v. 6 [21] allows the simultaneous inclusion in the code of both Rietveld and Pawley [22] routines or macros, therefore the difficulty is overcome by an alternative parameterisation of M3.

Table 1 – Identification of instruments according to experimental conditions and ancillary used. The geometry of the setup is either reflection Bragg–Brentano (*R*) or transmission capillary (*T*). Degrees are expressed in 2Θ and wavelength, in Å, corresponding to an energy of 30 keV.

Instrument	Manufacturer	Geometry	Wavelength	Spinning	Angular domain	Step
1	Panalytical	R	Cu $K\alpha_{1,2}$	Yes	10–90	0.038
2	Shimadzu	R	Cu $K\alpha_{1,2}$	No	10–89	0.02
3	Shimadzu	R	Cu $K\alpha_{1,2}$	Yes	10–89	0.02
4	Rigaku	R	Cu $K\alpha_{1,2}$	No	10–70	0.02
5	Rigaku	R	Cu $K\alpha_{1,2}$	No	26–88	0.025
7	Rigaku	R	Cu $K\alpha_{1,2}$	Yes	10–80	0.02
8	Bruker	R	Cu $K\alpha_{1,2}$	No	10–75	0.01
9	Bruker	T	Mo $K\alpha_1$	Yes	4–40	0.005659
10	ALBA	T	0.41290	Yes	2–30	0.02

The purpose of the present work is to try to establish, firstly, the discrepancies in the determination of M1 and M3 alite polymorphs, and secondly, the extent of the divergence in the quantification of the remaining phases, when several Portland cement samples are provided to different powder diffraction laboratories. The procedure used is similar to a small scale round robin exercise, giving the samples to finally treat by Rietveld analysis the experimental diffraction patterns with the help of Academic TOPAS.

This is a modest attempt to evaluate—from a practical point of view—the capacities of Brazilian laboratories equipped with powder diffraction instrumentation to carry out mineralogical quality control of cementitious materials with a view to a more ambitious objective such as the development of official engineering standards for the quantification of the mineral phases present in cementitious materials.

Experimental

Samples studied

The samples of cementitious materials were supplied by the Brazilian Association of Portland Cement. All types of cement used in Brazil, according to the typologies described in ABNT NBR 16 697, were used in this study. The figure attached to the name indicates the strength developed after 28 days of cure expressed in MPa: CP I-40 – Common Portland Cement; CP II-E-32 - Portland Cement Composite with Slag; CP II-F-32 – Portland Cement Composite with Filler; CP II-Z-32 – Portland Cement Composite with Pozzolan; CP III-40RS – Blast Furnace Portland Cement, Sulphate Resistant; CP IV-32 – Pozzolanic Portland Cement, and CP V-ARI – High Initial Strength Portland Cement. A more detailed description of these cements can be found in the publication of Natalli et al. [23].

Powder diffraction

Seven powder X-ray diffraction laboratories with nine instruments (seven of them Brazilian) and a synchrotron facility provided the diffraction patterns for this study. Most of the instruments were Bragg-Brentano configuration with Cu radiation. One instrument used was with transmission Debye–Scherrer geometry, Mo radiation and the specimen placed in a capillary tube of 0.5 mm internal diameter.

Sample holders for the Bragg–Brentano geometry were standard, except in one case where a zero-background (silicon single crystal cut) holder was used. The acquisitions were made with sample spinning in three cases, the rest were with static sample holders. In most cases the patterns were acquired between 10 and 80 2Θ degrees with steps of 0.02 degrees and counting the time per step until reaching approximately 10 kcps for the strongest peak.

For the Mo radiation acquisition the angular domain scanned was between 5 and 40 2Θ degrees with a step of 0.005659 degrees. Finally, the synchrotron pattern was acquired with a 30 keV energy that according to calibration with a Si standard provided a wavelength of 0.412896 Å. A summary of the experimental conditions for the diffraction patterns can be seen in Table 1.

X-ray fluorescence

X-ray fluorescence analyses were made at the facilities validated by INMETRO (Brazilian National Institute for Metrology StandardiZation and Industrial Quality) of the Brazilian Association of Portland Cement with the technique of cast slabs on a Rigaku ZSX Primus III+. Their results are based on a calibration curve made with twelve standards, including nine NIST primary standards and followed the guidelines of [24].

Data treatments

The Rietveld Analysis was carried out with the commercial package of TOPAS Academic version 6 [21]. For the basic statistical calculations, the Origin 8 package was used [25] and the guidelines of [26] were followed. The parameters included in the tables are defined below.

The average or mean as,

$$\bar{x} = \frac{1}{n}\sum x_i \tag{1}$$

The standard deviation as,

$$S = \frac{\sqrt{\sum (x_i - \bar{x})^2}}{n-1} \tag{2}$$

The standard error of mean as,

$$S_m = \frac{s}{\sqrt{n}} \tag{3}$$

The minimum value of the average with 95% of confidence, l_{95}, as

$$l = \bar{x} - t\left(1 - \frac{\alpha}{2}\right)\frac{s}{\sqrt{n}} \tag{4}$$

The maximum value of the average with 95% of confidence, u_{95}, as

$$u = \bar{x} + t\left(1 - \frac{\alpha}{2}\right)\frac{s}{\sqrt{n}} \tag{5}$$

The kurtosis parameter which is a measure of the combined weight of the tails relative to the rest of the distribution, g_2, is defined as,

$$\gamma_2 = \frac{n(n+1)}{(n-1)(n-2)(n-3)}\sum_{i=1}^{n}\left(\frac{x_i - \bar{x}}{s}\right)^4 - \frac{3(n-1)^2}{(n-2)(n-3)} \tag{6}$$

And finally, the average deviation also known as mean absolute deviation as,

$$S_a = \frac{\sum\left|x_i - \bar{x}\right|}{n} \tag{7}$$

Results and discussion

The refinements were carried out following the guidelines of McCusker et al. [27]. The peaks were shaped to full Voigt profile functions. The preferred orientation was corrected with the Mach–Dollase model [28]. TOPAS Academic was chosen for its robustness and flexibility that allows fine of tuning the refinement of crystalline phases in a very precise way. Furthermore, it also allows you to enter lines of code to determine the percentage composition of M3 in a non-standard way using a Pawley scheme.

For the structure of M1 the model of Dunstetter el al. [18] was used and for M3 the model of Nishi et al. [29]. For the second major component, belite, the crystal model of Mumme [30] was used, for the tricalcium aluminate the model of Mondal et al. [31] was used, for the cubic ferrite, the description of Colville et al. [32] and finally for the orthorhombic with Na content, the description of Nishi and Takeuchi [33]. The crystal structure model for calcite was taken from Graf [34], for portlandite the model of Henderson and Gutowsky [35], for periclase the model of Hazen [36] and for mullite the model of Ross and Prewitt [37]. As far as sulphates are concerned, for arcanite the model of McGinnety [38] was used, for langbeinite the model of Speer and Salje [39], for anhydrite the description of Hawthorne and Ferguson [40], for bassanite the description of Ballirano et al. [41], for gypsum, the structure reported by Schofield et al. [42] and for aphthitalite the crystal structure of Okada and Ossaka [43].

The complete script with the macro commands used for the refinements is available to any interested reader upon request from the authors. To have a broader view of the possibilities of this software the book of Dinnebier et al. [44] can be consulted.

The clinker sample, being less complex, was measured with three additional instruments – one of them with synchrotron radiation – to have a kind of reference. These commercial cement samples were chosen because they are the most used in Brazil. In principle, their mineral composition could in most cases be determined with relatively good accuracy. However, CP II-E can have substantial additions of slag, up to 34%, in addition both CP II-Z and CP IV contain pozzolanic additions, and CP III contains blast furnace slag. The carbonate material, also added, ranges from 6% to 25%, the latter being for the CP II-F. These additions imply a substantial increase in the non-crystalline fraction. From this it follows that in order to characterise a cementitious sample mineralogically, it will also be necessary to determine the portion of non-crystalline material. The tools for this task are well established [45], and some studies addressing this problem have been published [46,47], but this is outside the scope of this study. Here it is assumed that the presence of non-crystalline phases is negligible in the cements examined. Under this premise it is obvious that the percentages deduced for CaO and SiO_2 will not be the real ones. However, the relative proportion between the quantified crystalline phases will be real.

An example of an adjusted diffraction pattern for the clinker sample can be seen in Fig. 1 and enlarged views of the angular region between 28.5 and 35.5 2Θ degrees are shown in Figs. 2 and 3; the calculated patterns of phases M1 and M3 are superimposed on the experimental diffraction profiles. It is clearly seen that both phases are perfectly distinguishable and therefore can be quantified without any problem. A summary of the chemical composition obtained by X-ray fluorescence can be found in Table 2. The clinker sample whose mineralogical composition is shown in Table 3 was measured with ten instruments, including Mo and synchrotron radiation. The rest of the cement samples were measured with seven instruments and the results can be found in Tables 4–10. The percent compositions of main crystalline phases are compiled with some statistical indicators of the goodness of fit. These Tables also contain the chemical compositions in the form of oxides, deduced from the mineralogical composition. It was assumed for the minor oxides that magnesium oxide comes from periclase; CO_2 from calcite; water from bassanite, gypsum and portlandite; potassium oxide from langbeinite, arcanite and aphthitalite; and sodium oxide from aphthitalite.

The results between the different patterns is pretty consistent, but in order to have a more objective view of the statistical reality of the results, basic calculations of deviations, averages and variations between maximum and minimum values were made. After a careful examination of the tables, what is most apparent is a great disparity between the instruments with respect to the precision of the measurements. As mentioned above, the procedure to be followed to prepare the sample and analyse it in the diffractometer was left to the discretion of each laboratory. Discrepancies may therefore be due to the way the powder is placed in the sample holder, whether fixed or rotating, as well as the characteristics of the optics and detection system. In this regard, it is evident that instrument number four is the one that exhibits the worst performance. Perhaps it would have been necessary to exclude it

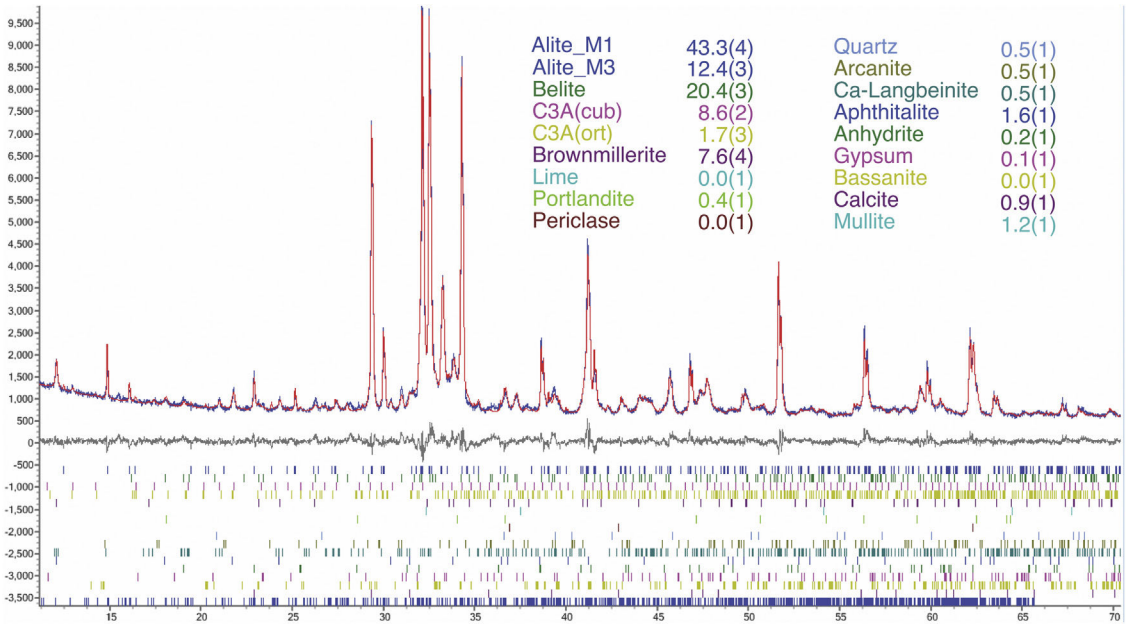

Fig. 1 – Rietveld refinement profile of the clinker studied, showing experimental, calculated and difference curves between 10 and 70 2Θ degrees. Intensity expressed as counts per second.

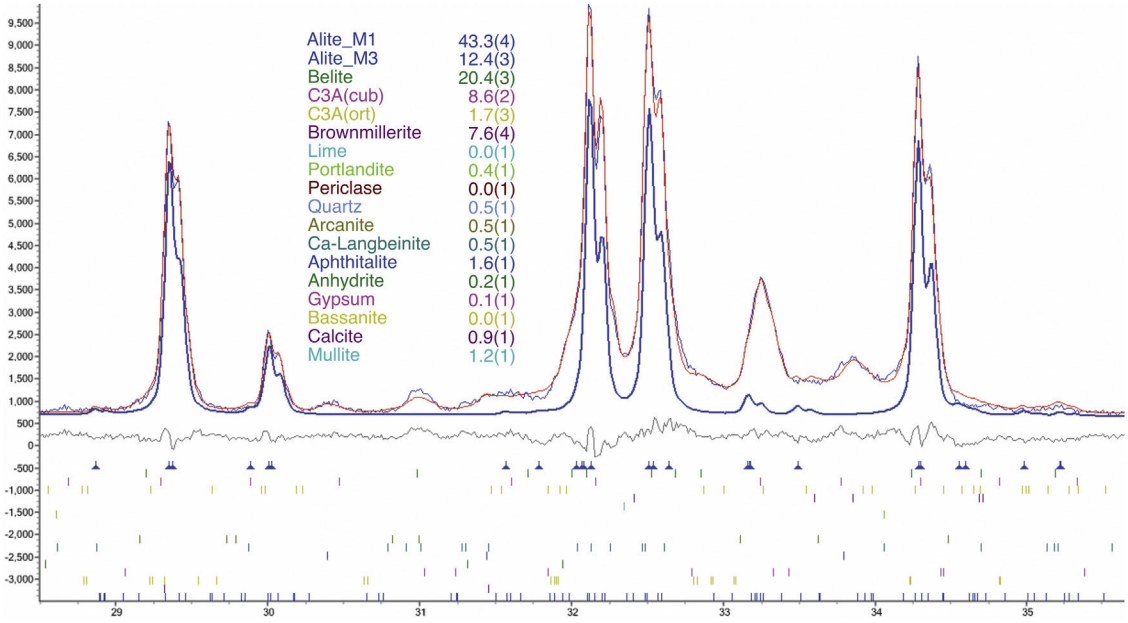

Fig. 2 – A detail of the Rietveld refinement curves on a restricted area, showing the contribution due to M1 polymorph. Abscissa expressed in 2Θ degrees and intensity as cps.

from the statistics, but it was kept in order to finally obtain a more representative view of the powder diffraction laboratories available in Brazil for the mineralogical analysis of cements.

Regarding the mean values obtained with their standard deviations, variations are observed for the main phases of M1 and M3, between 1 and almost 5 percentage points, with more important deviations for CP II specimens and clinker. Likewise, for the deduced percentages of CaO and SiO_2, the variations range between 0.4 and 1.1 percentage points. These values are within reason and are promising, since they indicate that with a more rigorous procedure following well-defined protocols, the precision would be more than acceptable. Therefore, it can be concluded in the first place that the determination of the polymorphs of alite is possible. However, to validate this and to what extent the results are reproducible, it would be necessary to use other software. This is a pending task for future development. Regarding the estimation of the chemical composition in the form of equivalent oxides from the mineralogical composition that was made to compare with the values measured with X-ray fluorescence, deviations can be observed due to the presence of non-crystalline material. The most notable

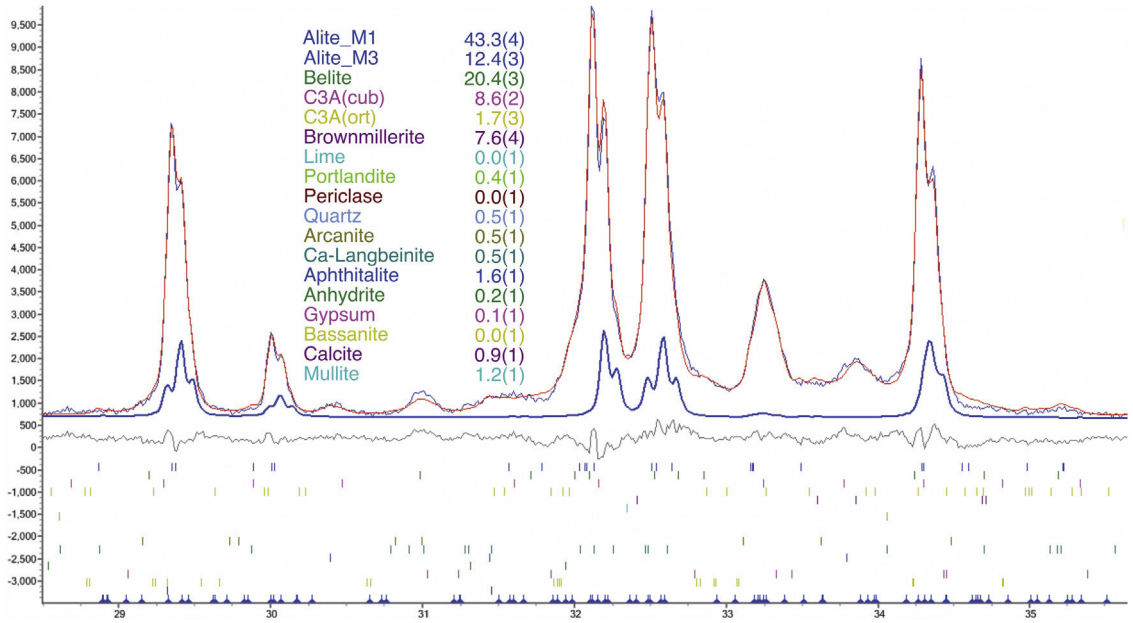

Fig. 3 – A detail of the Rietveld refinement curves on a restricted area, showing the contribution due to M3 polymorph. Abscissa expressed in 2Θ degrees and intensity as cps.

Table 2 – X-ray fluorescence results of the chemical analysis of main elements, expressed as oxides in percent to the last certain digit. The last row shows the loss on ignition in percent.

Component	Clinker	CP I-40	CP II E-32	CP II F-32	CP II Z-32	CP III-40 RS	CP IV-32	CP V ARI
CaO	64.44	59.39	53.34	59.93	50.45	49.95	34.03	59.16
SiO_2	20.87	19.97	22.79	17.11	22.04	24.50	35.91	18.13
Al_2O_3	5.94	5.02	6.34	4.24	5.43	8.06	12.17	4.51
Fe_2O_3	3.00	3.20	2.47	2.30	3.02	1.99	3.70	2.71
SO_3	2.12	2.56	2.91	2.77	3.78	3.33	2.20	3.43
MgO	1.01	5.31	2.43	5.08	5.22	5.49	4.07	6.36
K_2O	1.06	0.48	0.94	0.81	1.16	0.72	1.64	0.80
Na_2O	0.20	0.12	0.37	0.19	0.22	0.26	0.37	0.12
TiO_2	0.25	0.27	0.31	0.20	0.25	0.41	0.62	0.22
SrO	0.09	0.13	0.27	0.04	0.07	0.07	0.04	0.06
P_2O_5	0.10	0.12	0.14	0.10	0.14	0.08	0.10	0.17
MnO	0.05	0.15	0.35	0.12	0.93	0.40	0.11	0.16
Total	99.13	98.48	98.23	98.47	98.60	98.40	98.86	98.18
LOI	0.32	1.75	5.56	5.58	5.89	3.11	3.89	2.36

discrepancies are observed for CP III and CP IV, which seem to indicate the presence of a higher proportion of slag. This brings up the issue of determining the non-crystalline portion in cementitious materials, which is becoming increasingly important since the new regulations allow greater additions of by-products from industrial plants. Although, as mentioned above, the determination procedures are well established, no inter-laboratory round robin has been carried out systematically to verify the statistical deviations and to propose a standard routine for this purpose. This is another pending task.

It would also be convenient at this point to remember the proposal of several authors [12,48], to return to the classical method of chemical extraction with KOH and sucrose to retain calcium silicates and periclase on one hand and on the other with salicylic acid and methanol to remove calcium silicates and free lime, leaving a residue of interstitial phases aluminate and ferrite as well as minor phases periclase and alkali sulphates. These are relatively simple analytical procedures that could certainly improve the accuracy of the mineralogical determination.

Table 3 – The Clinker mass percent composition of main phases and the equivalent oxide composition in columns 1–10 for the diffraction instruments used. Figures are represented with error in brackets affecting the last digit. The columns of the statistical indicators labelled as *m* for mean, *s* for standard deviation, s_m for standard deviation of mean, l_{95} and u_{95} for lower and upper limits of the 95% confidence intervals of mean, g_2 for the kurtosis parameter and s_a for the mean absolute deviation. The last two rows contain the statistical indicators for the Rietveld refinements.

Phase/Oxide	1	2	3	4	5	6	7	8	9	10	*m*	*s*	s_m	l_{95}	u_{95}	g_2	s_a
Alite (total)	55.7(4)	58.5(9)	59.7(8)	52(2)	62(1)	61.0(7)	59.5(8)	57.0(6)	54.2(5)	55.7(5)	57.53	3.28	1.04	55.19	59.88	−0.49	2.67
Alite (M1)	43.3(4)	43.7(9)	44.8(8)	34(2)	47(1)	40.9(7)	43.4(8)	39.8(6)	40.7(5)	44.1(5)	42.21	3.42	1.208	39.77	44.66	2.04	2.58
Alite (M3)	12.4(3)	14.8(8)	14.9(8)	17(2)	15,5(8)	20.0(7)	16.1(8)	17.2(5)	13.6(5)	11.6(4)	15.32	2.48	0.78	13.55	17.10	0.23	1.86
Belite	20.4(3)	17.0(5)	16.4(5)	18(2)	11.9(6)	16.0(4)	17.2(5)	14.1(4)	20.8(3)	19.2(3)	17.10	2.73	0.86	15.15	19.05	0.08	1.99
C3A (cub.)	8.6(2)	8.1(4)	8.6(4)	7(1)	9.2(47)	8.7(3)	7.2(4)	9.9(3)	10.3(3)	9.7(2)	8.72	1.14	0.36	7.90	9.54	−0.40	0.85
C3A (ort.)	1.7(3)	1.7(5)	1.4(4)	2(2)	1.8(8)	1.5(4)	2.3(5)	2.0(4)	1.2(3)	1.2(3)	1.67	0.35	0.11	1.43	1.92	−0.34	0.27
Brownmillerite	7.6(4)	7.9(6)	7.3(5)	12(2)	7.2(8)	6.9(4)	8.4(6)	6.2(4)	8.1(4)	8.3(4)	7.97	1.50	0.48	6.90	9.05	5.28	0.94
Lime	0.0(1)	0.2(1)	0.2(1)	0.5(2)	0.0(1)	0.1(1)	0.2(1)	0.0(1)	0.1(1)	0.1(1)	0.14	0.15	0.05	0.03	0.24	2.80	0.11
Portlandite	0.4(1)	0.3(1)	0.3(1)	1.2(3)	1.8(5)	0.6(1)	0.1(1)	0.3(1)	0.3(1)	0.2(1)	0.56	0.54	0.17	0.18	0.95	2.81	0.39
Periclase	0.0(1)	0.1(1)	0.0(1)	1.5(4)	0.0(1)	0.1(1)	0.0(1)	0.0(1)	0.1(1)	0.1(1)	0.19	0.47	0.15	0.00	0.53	9.77	0.27
Quartz	0.5(1)	0.4(1)	0.3(1)	0.0(3)	0.2(1)	0.4(1)	0.7(1)	1.0(1)	0.4(1)	0.5(1)	0.44	0.27	0.09	0.24	0.63	2.14	0.18
Arcanite	0.5(1)	0.5(2)	0.3(2)	0.3(5)	0.3(3)	0.2(1)	0.0(2)	0.8(2)	0.1(1)	0.1(1)	0.30	0.23	0.07	0.14	0.47	0.72	0.17
Langbeinite	0.5(1)	0.7(2)	0.6(2)	0.0(7)	0.0(2)	0.4(1)	0.9(2)	1.7(2)	0.5(1)	0.9(2)	0.62	0.49	0.15	0.27	0.97	1.86	0.34
Aphthitalite	1.6(1)	1.6(2)	1.7(1)	1.0(4)	1.6(2)	1.5(1)	1.6(1)	1.7(1)	1.0(1)	1.2(1)	1.46	0.27	0.09	1.26	1.66	−0.36	0.23
Anhydrite	0.2(1)	0.3(1)	0.2(1)	0.0(3)	0.8(5)	0.2(1)	0.3(1)	0.6(1)	0.1(1)	0.1(1)	0.30	0.26	0.08	0.11	0.48	120	0.18
Gypsum	0.1(1)	0.2(1)	0.2(1)	0.3(5)	0.5(4)	0.0(1)	0.0(1)	0.6(2)	0.2(1)	0.2(1)	0.24	0.19	0.06	0.10	0.38	0.90	0.14
Bassanite	0.0(1)	0.1(1)	0.0(1)	0.5(6)	0.0(3)	0.0(1)	0.0(1)	0.1(1)	0.3(1)	0.2(1)	0.11	0.17	0.05	0.00	0.23	1.05	0.14
Calcite	0.9(1)	1.1(2)	1.5(2)	2.3(5)	1.0(3)	1.3(2)	0.8(2)	1.0(1)	1.0(1)	0.9(1)	1.19	0.44	0.14	0.87	1.50	5.00	0.31
Mullite	1.2(2)	1.3(2)	1.2(2)	2.6(9)	1.1(4)	1.0(2)	0.6(2)	3.0(2)	1.2(2)	1.3(2)	1.46	0.73	0.23	0.94	1.98	1.41	0.53
CaO	65.2(2)	65.3(3)	65.8(3)	64(1)	66.5(5)	66.4(3)	65.8(3)	62.9(3)	65.6(2)	65.3(2)	65.25	1.14	0.36	64.43	66.07	0.82	0.81
SiO_2	22.6(2)	22.1(3)	22.1(2)	20.5(8)	21.1(4)	22.3(2)	22.5(2)	21.7(2)	22.2(2)	22.2(2)	21.94	0.65	0.21	21.47	22.40	1.64	0.49
Al_2O_3	5.7(2)	6.1(3)	5.8(3)	8(1)	7.4(6)	5.8(3)	5.0(3)	7.0(3)	6.7(2)	6.5(2)	6.44	0.98	0.31	573	7.14	0.52	0.76
Fe_2O_3	3.4(2)	2.9(4)	2.9(3)	3(1)	1.3(6)	2.6(3)	3.7(4)	3.2(4)	2.9(2)	3.1(3)	2.89	0.64	0.20	2.44	3.35	4.66	0.39
SO_3	1.4(1)	1.5(2)	1.4(1)	1.0(6)	1.7(4)	1.1(1)	1.4(2)	2.5(2)	1.1(1)	1.3(1)	1.45	0.43	0.14	1.14	1.76	4.37	0.28
MgO	0.0(1)	0.1(1)	0.0(1)	1.5(4)	0.0(1)	0.1(1)	0.02(1)	0.0(1)	0.1(1)	0.1(1)	0.19	0.47	0.15	0.00	0.53	9.77	0.27
CO_2	0.4(1)	0.5(1)	0.6(1)	1.0(2)	0.4(1)	0.6(1)	0.4(1)	0.4(1)	0.4(1)	0.4(1)	0.52	0.19	0.06	0.38	0.66	5.00	0.13
H_2O	0.1(1)	0.1(1)	0.1(1)	0.3(1)	0.5(1)	0.1(0)	0.04(3)	0.2(1)	0.1(1)	0.1(1)	0.19	0.15	0.05	0.08	0.30	2.50	0.11
K_2O	0.9(1)	1.0(1)	0.9(1)	0.5(4)	0.6(2)	0.7(1)	0.9(1)	1.6(1)	0.6(1)	0.8(1)	0.86	0.32	0.10	0.63	1.09	3.59	0.22
Na_2O	0.3(1)	0.3(1)	0.3(1)	0.2(1)	0.32(5)	0.3(0)	0.32(2)	0.3(1)	0.2(1)	0.2(1)	0.29	0.05	0.02	0.25	0.32	−0.36	0.04
Rwp	5.60	11.70	10.89	12.79	12.05	9.63	11.37	7.37	8.97	8.27							
GOF	1.73	1.84	1.71	3.24	2.75	2.74	2.85	2.90	2.37	3.05							

Table 4 – CP I-40 mass percent composition of main phases and the equivalent oxide composition in columns 1–7 for the diffraction instruments used. Figures are represented with error in brackets affecting the last digit. The columns of the statistical indicators labelled as m for mean, *s* for standard deviation, s_m for standard deviation of mean, l_{95} and u_{95} for lower and upper limits of the 95% confidence intervals of mean, g_2 for the kurtosis parameter and s_a for the mean absolute deviation. The last two rows contain the statistical indicators for the Rietveld refinements.

Phase/Oxide	1	2	3	4	5	6	7	*m*	*s*	s_m	l_{95}	u_{95}	g_2	s_a
Alite (total)	59.9(4)	56.0(8)	57.6(7)	55(2)	58.4(8)	59.3(6)	60(1)	57.93	1.98	0.75	56.10	59.76	−0.76	1.59
Alite (M1)	42.8(4)	39.2(8)	41.2(7)	35(2)	38.8(8)	38.8(6)	33(1)	38.37	3.46	1.31	35.16	41.57	−0.60	2.60
Alite (M3)	17.0(4)	16.8(7)	16.3(7)	20(1)	19.5(7)	20.5(6)	27(1)	19.57	3.57	1.35	16.26	22.87	2.57	2.46
Belite	12.4(3)	13.9(5)	13.3(5)	9(1)	12.9(5)	14.0(4)	13.5(6)	12.70	1.78	0.67	11.05	14.34	4.86	1.18
C3A (cub.)	3.7(2)	3.3(8)	3.0(3)	3.5(8)	3.3(4)	3.3(3)	2.7(5)	3.25	0.33	0.12	2.95	3.55	0.86	0.24
C3A (ort.)	0.6(2)	0.3(8)	0.3(3)	0.4(6)	0.2(4)	0.2(3)	0.2(5)	0.30	0.15	0.06	0.16	0.44	139	0.11
Brownmillerite	10.1(4)	10.7(5)	10.6(5)	14.4(8)	9.9(7)	9.8(4)	8.8(5)	10.61	1.77	0.67	8.97	12.25	4.75	1.10
Lime	0.1(1)	0.2(8)	0.3(1)	0.2(2)	0.1(1)	0.2(1)	0.3(1)	0.20	0.08	0.03	0.13	0.27	−0.21	0.06
Portlandite	0.8(1)	0.6(1)	0.5(1)	1.4(3)	1.5(2)	0.9(1)	0.2(1)	0.85	0.47	0.18	0.42	1.28	−0.74	0.36
Periclase	4.4(1)	5.0(1)	4.8(1)	5.9(4)	3.8(1)	4.3(1)	4.3(2)	4.66	0.68	0.26	4.03	5.29	1.89	0.49
Quartz	0.2(1)	0.5(1)	0.5(1)	0.0(2)	0.5(1)	0.2(1)	0.4(1)	0.34	0.20	0.07	0.16	0.52	−0.32	0.16
Arcanite	0.7(1)	0.7(2)	0.7(2)	0.2(4)	0.4(2)	0.5(1)	1.7(3)	0.72	0.50	0.19	0.26	1.18	4.05	0.31
Langbeinite	0.4(1)	0.7(8)	0.7(2)	0.0(5)	0.0(2)	0.5(1)	0.7(2)	0.43	0.31	0.12	0.15	0.72	−1.37	0.25
Aphthitalite	0.7(1)	0.5(8)	0.5(1)	0.1(3)	0.4(4)	0.3(1)	0.4(2)	0.42	0.19	0.07	0.25	0.59	1.97	0.13
Anhydrite	0.3(1)	0.4(1)	0.5(1)	0.5(4)	1.1(3)	0.2(1)	0.2(1)	0.47	0.32	0.12	0.17	0.76	4.77	0.20
Gypsum	1.8(1)	2.3(1)	2.3(1)	1.6(5)	3.3(4)	1.7(1)	1.6(1)	2.10	0.63	0.24	1.52	2.68	2.58	0.47
Bassanite	1.7(1)	1.4(2)	1.4(1)	1.6(5)	2.1(2)	1.7(1)	1.8(2)	1.68	0.26	0.10	1.45	1.92	0.83	0.19
Calcite	1.3(1)	2.1(2)	1.8(2)	3.0(4)	1.3(2)	1.8(1)	3.0(2)	2.05	0.71	0.27	1.39	2.71	−1.32	0.56
Mullite	1.0(2)	1.2(2)	1.2(2)	3.7(8)	0.7(2)	0.7(2)	0.5(2)	1.29	1.10	0.41	0.28	2.31	5.54	0.69
CaO	62.1(2)	60.8(3)	61.1(3)	59.6(8)	62.3(3)	62.7(2)	62.0(4)	61.54	1.07	0.41	60.55	62.53	0.34	0.86
SiO_2	20.6(1)	20.5(2)	20.6(2)	18.5(7)	20.5(3)	20.9(2)	20.9(3)	20.36	0.85	0.32	19.57	21.15	5.83	0.54
Al_2O_3	3.5(2)	3.8(2)	3.4(3)	8(1)	2.9(4)	3.0(2)	2.4(4)	3.87	1.90	0.72	2.11	5.63	5.81	1.20
Fe_2O_3	4.5(2)	4.4(3)	4.6(3)	4(1)	4.4(6)	4.3(3)	4.0(4)	4.27	0.34	0.13	3.96	4.59	1.06	0.26
SO_3	2.7(1)	2.9(1)	3.0(2)	2.0(5)	3.8(3)	2.5(1)	3.1(2)	2.88	0.56	0.21	2.36	3.40	1.29	0.39
MgO	4.4(1)	4.9(1)	4.8(1)	5.9(4)	3.8(1)	4.3(1)	4.3(2)	4.66	0.68	0.26	4.03	5.29	1.89	0.49
CO_2	0.6(1)	0.9(1)	0.8(1)	1.3(2)	0.5(1)	0.8(1)	1.3(2)	0.90	0.31	0.12	0.61	1.19	−1.32	0.25
H_2O	0.7(1)	0.7(1)	0.7(1)	0.8(1)	1.2(1)	0.7(1)	0.5(1)	0.75	0.22	0.08	0.55	0.95	4.33	0.13
K_2O	0.7(1)	0.8(1)	0.8(1)	0.1(3)	0.4(2)	0.6(1)	1.3(3)	0.70	0.39	0.15	0.34	1.06	0.56	0.29
Na_2O	0.1(1)	0.1(1)	0.1(1)	0.0(1)	0.08(4)	0.1(1)	0.08(4)	0.08	0.04	0.01	0.05	0.12	1.97	0.03
Rwp	5.61	11.25	11.04	11.34	8.72	8.93	14.57							
GOF	1.78	1.81	1.78	2.73	1.96	2.73	3.68							

Table 5 – CP II-E-32 mass percent composition of main phases and the equivalent oxide composition in columns 1–7 for the diffraction instruments used. Figures are represented with error in brackets affecting the last digit. The columns of the statistical indicators labelled as *m* for mean, *s* for standard deviation, s_m for standard deviation of mean, l_{95} and u_{95} for lower and upper limits of the 95% confidence intervals of mean, g_2 for the kurtosis parameter and s_a for the mean absolute deviation. The last two rows contain the statistical indicators for the Rietveld refinements.

Phase/Oxide	1	2	3	4	5	6	7	*m*	*s*	s_m	l_{95}	u_{95}	g_2	s_a
Alite (total)	47.7(7)	47.05	47(1)	44(2)	44(1)	51(1)	50(1)	47.13	2.55	0.96	44.77	49.49	−1.03	1.89
Alite (M1)	19.1(7)	19(1)	19(1)	20(2)	20(1)	21(1)	23(1)	20.33	1.55	0.59	18.89	21.77	3.22	1.10
Alite (M3)	28.5(7)	28(1)	27(1)	24(2)	24(1)	30(1)	26(1)	26.80	2.28	0.86	24.70	28.90	−1.19	1.85
Belite	12.1(6)	11.5(8)	11.9(7)	14(2)	15.7(9)	11.5(6)	11.6(7)	12.57	1.59	0.60	11.10	14.05	2.21	1.22
C3A (cub.)	0.5(4)	0.3(5)	0.4(4)	0.3(1)	1.2(9)	0.4(5)	0.4(4)	0.49	0.30	0.11	0.21	0.78	5.67	0.19
C3A (ort.)	2.8(5)	2.8(6)	2.8(6)	3(1)	1.9(9)	3.5(6)	2.0(5)	2.71	0.59	0.22	2.16	3.25	-0.73	0.43
Brownmillerite	9.1(7)	8.0(8)	8.4(8)	12(2)	7(1)	7.5(6)	8.5(7)	8.64	1.63	0.62	7.13	10.15	3.64	1.09
Lime	0.0(1)	0.0(1)	0.0(1)	0.4(3)	0.0(1)	0.0(1)	0.1(1)	0.07	0.14	0.05	0.00	0.20	6.24	0.09
Portlandite	0.3(2)	0.2(1)	0.1(1)	0.0(3)	0.9(4)	0.7(2)	0.3(1)	0.38	0.31	0.12	0.09	0.66	−0.30	0.24
Periclase	0.0(1)	0.0(2)	0.0(2)	0.8(4)	0.0(1)	0.0(1)	0.0(2)	0.13	0.31	0.12	0.00	0.42	6.91	0.20
Quartz	1.3(1)	1.4(2)	2.1(2)	1.4(3)	2.4(2)	1.4(1)	1.8(2)	1.68	0.43	0.16	1.28	2.08	−0.76	0.36
Arcanite	1.8(2)	1.5(3)	1.3(3)	1.8(7)	1.8(4)	1.5(3)	1.2(3)	1.56	0.23	0.09	1.34	1.78	−1.59	0.19
Langbeinite	2.5(2)	2.9(3)	2.8(3)	0.3(5)	0.6(4)	2.6(2)	2.5(2)	2.04	1.08	0.41	1.04	3.04	−0.79	0.89
Aphthitalite	1.3(2)	1.2(3)	1.2(2)	1.2(6)	1.1(3)	1.1(2)	0.9(2)	1.16	0.13	0.05	1.04	1.27	1.84	0.08
Anhydrite	0.8(1)	1.1(2)	1.2(2)	0.0(3)	1.2(4)	1.1(1)	2.1(1)	1.08	0.61	0.23	0.51	1.64	2.36	0.38
Gypsum	3.1(2)	3.9(2)	3.4(2)	3.0(5)	4.3(6)	2.6(1)	2.4(2)	3.26	0.69	0.26	2.62	3.90	−0.91	0.55
Bassanite	0.6(2)	0.5(2)	0.2(1)	3.2(7)	1.2(4)	0.4(2)	0.2(2)	0.90	1.05	0.40	0.00	1.87	4.90	0.72
Calcite	15.0(3)	16.1(5)	16.1(4)	13.3(9)	15.9(6)	14.7(4)	15.5(4)	15.24	1.01	0.38	14.30	16.17	1.34	0.77
Mullite	0.9(3)	1.5(4)	1.1(3)	1.4(8)	0.6(4)	0.3(3)	0.9(3)	0.97	0.41	0.15	0.60	1.35	−0.79	0.31
CaO	59.9(3)	59.3(5)	59.4(5)	59(1)	59.9(6)	61.3(4)	60.6(4)	59.95	0.78	0.30	59.22	60.67	0.22	0.58
SiO_2	18.3(3)	18.1(3)	18.9(3)	18.1(7)	19.6(5)	18.9(3)	19.2(3)	18.73	0.57	0.22	18.20	19.26	−0.97	0.46
Al_2O_3	2.7(4)	2.7(5)	2.3(4)	5(1)	2.6(7)	2.2(4)	2.3(4)	2.84	0.91	0.34	2.00	3.68	5.96	0.57
Fe_2O_3	4.3(5)	4.1(6)	4.5(6)	4(1)	2.8(8)	3.7(5)	4.0(5)	3.94	0.55	0.21	3.43	4.44	3.13	0.37
SO_3	4.7(2)	5.1(3)	4.7(3)	4.7(7)	5.0(5)	4.2(2)	4.3(2)	4.68	0.31	0.12	4.40	4.97	−0.89	0.22
MgO	0.0(1)	0.0(2)	0.0(2)	0.8(4)	0.0(1)	0.0(2)	0.0(-)	0.13	0.31	0.12	0.00	0.42	6.91	0.20
CO_2	6.6(1)	7.1(2)	7.1(2)	5.8(4)	7.0(3)	6.4(2)	6.8(2)	6.70	0.44	0.17	6.29	7.11	1.37	0.34
H_2O	0.8(1)	0.9(1)	0.8(1)	0.8(1)	1.2(1)	0.7(1)	0.58(4)	0.83	0.19	0.07	0.66	1.01	2.40	0.13
K_2O	2.4(2)	2.4(2)	2.2(2)	1.4(5)	1.6(3)	2.2(2)	2.0(2)	2.04	0.38	0.14	1.69	2.40	−1.30	0.31
Na_2O	0.3(1)	0.2(1)	0.2(1)	0.2(1)	0.22(6)	0.2(1)	0.18(4)	0.23	0.02	0.01	0.20	0.25	1.91	0.02
Rwp	7.72	13.69	12.82	10.19	10.93	11.42	13.19							
GOF	2.43	2.27	2.13	2.45	2.11	3.64	3.57							

Table 6 – CP II-F-32 mass percent composition of main phases and the equivalent oxide composition in columns 1–7 for the diffraction instruments used. Figures are represented with error in brackets affecting the last digit. The columns of the statistical indicators labelled as *m* for mean, *s* for standard deviation, s_m for standard deviation of mean, l_{95} and u_{95} for lower and upper limits of the 95% confidence intervals of mean, g_2 for the kurtosis parameter and s_a for the mean absolute deviation. The last two rows contain the statistical indicators for the Rietveld refinements.

Phase/Oxide	1	2	3	4	5	6	7	*m*	*s*	s_m	l_{95}	u_{95}	g_2	s_a
Alite (total)	60.7(6)	60.9(9)	61.8(9)	61(2)	59(1)	61.3(8)	59.6(9)	60.70	0.88	0.33	59.89	61.52	−0.94	0.68
Alite (M1)	30.9(6)	34.5(9)	34.7(9)	43(2)	35(1)	31.2(8)	34.1(9)	34.74	3.99	1.51	31.05	38.43	3.88	2.36
Alite (M3)	29.8(6)	26.4(9)	27.1(9)	18(2)	25(1)	30.0(8)	25.5(8)	25.97	3.98	1.50	22.29	29.64	2.31	2.71
Belite	5.1(3)	3.3(4)	3.5(5)	8(1)	6.3(6)	5.5(5)	5.0(5)	5.28	1.69	0.64	3.72	6.84	0.49	1.20
C3A (cub.)	4.5(2)	4.3(4)	4.7(4)	4(1)	4.5(7)	4.8(4)	4.1(4)	4.45	0.31	0.12	4.16	4.74	0.05	0.24
C3A (ort.)	0.2(3)	0.2(4)	0.1(4)	0.0(1)	0.0(1)	0.0(4)	0.0(4)	0.06	0.09	0.03	0.00	0.15	−1.23	0.07
Brownmillerite	7.8(5)	7.3(6)	7.3(6)	8(1)	6.2(8)	6.6(5)	7.6(6)	7.23	0.58	0.22	6.69	7.77	−0.43	0.45
Lime	0.0(1)	0.1(1)	0.1(1)	1.0(2)	0.1(1)	0.1(1)	0.2(1)	0.23	0.34	0.13	0.00	0.54	5.97	0.22
Portlandite	2.1(2)	2.0(2)	2.0(2)	0.0(3)	1.6(3)	2.4(2)	1.4(1)	1.64	0.80	0.30	0.90	2.38	3.44	0.55
Periclase	3.5(1)	5.4(2)	4.5(2)	3.6(3)	3.0(2)	4.3(1)	4.8(2)	4.18	0.83	0.31	3.42	4.95	−1.13	0.68
Quartz	0.6(1)	1.1(1)	0.7(1)	0.2(2)	0.6(1)	0.9(1)	0.8(1)	0.70	0.28	0.11	0.44	0.96	0.80	0.20
Arcanite	0.8(1)	0.3(2)	0.5(2)	0.2(5)	0.7(2)	0.5(2)	0.2(1)	0.45	0.23	0.09	0.24	0.67	−1.33	0.18
Langbeinite	0.3(1)	0.6(2)	0.6(2)	0.0(4)	0.1(2)	0.2(2)	0.6(2)	0.35	0.26	0.10	0.11	0.59	−1.91	0.22
Aphthitalite	0.6(1)	0.7(2)	0.8(2)	0.4(3)	0.4(2)	0.4(1)	0.3(1)	0.52	0.21	0.08	0.32	0.71	−1.68	0.18
Anhydrite	0.2(1)	0.2(1)	0.2(1)	0.0(3)	1.1(3)	0.1(1)	0.3(1)	0.31	0.37	0.14	0.00	0.65	5.53	0.24
Gypsum	0.4(1)	0.7(1)	0.8(1)	0.5(5)	1.8(5)	0.3(1)	0.3(1)	0.66	0.52	0.20	0.18	1.15	3.89	0.36
Bassanite	2.0(1)	1.8(2)	1.9(2)	3.6(6)	3.6(4)	2.1(2)	1.9(2)	2.40	0.81	0.31	1.65	3.15	−0.90	0.67
Calcite	10.1(2)	9.8(3)	9.5(3)	7.3(5)	10.1(4)	10.3(3)	12.3(3)	9.93	1.48	0.56	8.57	11.30	2.56	0.90
Mullite	0.9(2)	1.1(2)	1.0(2)	2.2(7)	0.3(3)	0.3(2)	0.4(2)	0.89	0.68	0.26	0.26	1.52	2.01	0.48
CaO	62.8(3)	61.3(4)	62.1(3)	63.1(9)	62.9(5)	63.2(3)	62.4(3)	62.55	0.66	0.25	61.94	63.17	0.70	0.52
SiO_2	18.6(2)	18.5(2)	18.5(2)	19.8(7)	18.5(4)	19.0(2)	18.3(2)	18.76	0.50	0.19	18.29	19.22	3.42	0.37
Al_2O_3	3.2(3)	3.2(3)	3.0(3)	5(1)	2.7(5)	2.6(3)	2.8(3)	3.18	0.71	0.27	2.52	3.84	4.73	0.45
Fe_2O_3	3.6(3)	3.6(4)	3.6(4)	3(1)	2.7(7)	3.1(4)	3.3(4)	3.23	0.46	0.17	2.80	3.65	−1.38	0.38
SO_3	2.2(1)	2.1(2)	2.3(2)	2.5(5)	4.0(4)	1.8(2)	1.8(2)	2.41	0.74	0.28	1.72	3.10	4.93	0.48
MgO	3.5(1)	5.4(2)	4.5(2)	3.6(3)	3.0(2)	4.3(1)	4.8(2)	4.18	0.83	0.31	3.42	4.95	−1.13	0.68
CO_2	4.4(1)	4.3(1)	4.2(1)	3.2(2)	4.4(2)	4.5(1)	5.4(1)	4.37	0.65	0.25	3.77	4.97	2.56	0.40
H_2O	0.7(1)	0.7(1)	0.8(1)	0.3(1)	1.0(1)	0.8(1)	0.51(4)	0.69	0.21	0.08	0.49	0.88	0.77	0.16
K_2O	0.7(1)	0.6(1)	0.7(1)	0.2(3)	0.5(2)	0.5(1)	0.5(1)	0.55	0.18	0.07	0.38	0.71	0.37	0.14
Na_2O	0.1(1)	0.1(1)	0.2(1)	0.1(1)	0.07(3)	0.1(1)	0.05(3)	0.10	0.04	0.02	0.06	0.14	−1.68	0.04
Rwp	7.66	13.20	12.88	13.58	12.19	12.12	13.43							
GOF	2.28	2.11	2.06	3.18	3.00	3.72	3.52							

Table 7 – CP II-Z-32 mass percent composition of main phases and the equivalent oxide composition in columns 1 to 7 for the diffraction instruments used. Figures are represented with error in brackets affecting the last digit. The columns of the statistical indicators labelled as m for mean, s for standard deviation, s_m for standard deviation of mean, l_{95} and u_{95} for lower and upper limits of the 95% confidence intervals of mean, g_2 for the kurtosis parameter and s_a for the mean absolute deviation. The last two rows contain the statistical indicators for the Rietveld refinements.

Phase/Oxide	1	2	3	4	5	6	7	*m*	s	s_m	l_{95}	u_{95}	g_2	s_a
Alite (total)	48.8(5)	48(1)	48.3(9)	44(2)	45(1)	47.8(9)	46(1)	47.02	1.71	0.65	45.44	48.60	−1.27	1.45
Alite (M1)	22.0(5)	21(1)	22.0(9)	30(2)	18.1(1)	20.2(9)	23(1)	22.36	3.84	1.45	18.81	25.91	3.78	2.38
Alite (M3)	26.8(5)	27(1)	26.3(9)	14(2)	25(1)	27.6(9)	24(1)	24.66	4.83	1.83	20.19	29.13	5.26	3.32
Belite	9.0(3)	8.0(6)	8.4(5)	11(1)	7.6(6)	9.9(6)	10.1(6)	9.17	1.25	0.47	8.02	10.33	−1.12	1.02
C3A (cub.)	3.8(2)	2.9(3)	2.9(4)	3.4(8)	2.7(6)	3.3(4)	2.7(4)	3.12	0.40	0.15	2.75	3.49	−0.35	0.33
C3A (ort.)	0.0(2)	0.0(4)	0.0(4)	0.0(8)	0.0(1)	0.0(4)	0.0(5)	0.01	0.01	0.01	0.00	0.02	7.00	0.01
Brownmillerite	8.0(4)	8.5(7)	8.3(6)	11(2)	9(1)	6.7(5)	7.5(6)	8.40	1.29	0.49	7.21	9.59	2.24	0.86
Lime	0.0(1)	0.0(1)	0.1(1)	0.4(2)	0.0(1)	0.0(1)	0.1(1)	0.12	0.14	0.05	0.00	0.25	4.62	0.09
Portlandite	1.5(1)	1.4(2)	1.1(2)	0.4(3)	2.2(4)	1.9(2)	1.1(2)	1.38	0.58	0.22	0.84	1.92	0.53	0.42
Periclase	4.3(1)	3.8(2)	4.1(2)	5.6(4)	4.6(2)	4.2(1)	4.0(2)	4.38	0.61	0.23	3.82	4.94	3.22	0.43
Quartz	6.6(1)	7.3(2)	7.3(2)	6.0(4)	10.0(3)	8.4(2)	7.8(2)	7.66	1.31	0.49	6.45	8.87	1.02	0.96
Arcanite	1.6(2)	1.3(2)	1.1(2)	0.5(4)	1.8(3)	0.9(2)	0.4(2)	1.08	0.52	0.20	0.60	1.56	−1.23	0.41
Langbeinite	0.8(2)	0.6(2)	0.5(2)	0.0(4)	0.4(4)	0.5(2)	0.7(2)	0.50	0.28	0.10	0.25	0.76	1.05	0.20
Aphthitalite	0.3(1)	0.2(2)	0.3(2)	0.2(3)	0.2(3)	0.1(2)	0.3(2)	0.22	0.08	0.03	0.15	0.30	−0.30	0.06
Anhydrite	0.4(1)	0.3(1)	0.3(1)	0.0(3)	1.5(4)	0.4(1)	0.5(1)	0.49	0.49	0.19	0.04	0.95	5.28	0.30
Gypsum	5.3(1)	5.5(2)	5.8(2)	4.6(4)	5.1(6)	5.2(2)	6.2(2)	5.39	0.51	0.19	4.91	5.86	0.15	0.39
Bassanite	1.2(1)	1.1(2)	1.1(2)	2.9(6)	1.7(4)	1.1(1)	0.9(2)	1.43	0.70	0.27	0.78	2.08	4.07	0.51
Calcite	6.8(2)	9.1(3)	8.1(3)	7.0(5)	6.2(4)	7.9(2)	8.9(3)	7.73	1.08	0.41	6.73	8.73	−1.44	0.88
Mullite	1.4(2)	1.8(3)	2.1(3)	2.5(8)	1.6(4)	1.5(3)	2.4(3)	1.90	0.41	0.16	1.52	2.28	−1.76	0.35
CaO	55.2(3)	54.9(5)	54.7(4)	54.4(9)	52.2(6)	55.0(4)	54.5(4)	54.41	1.01	0.38	53.47	55.35	5.23	0.64
SiO_2	23.0(2)	23.3(3)	23.5(3)	22.2(7)	25.0(5)	24.9(3)	24.2(3)	23.75	1.03	0.39	22.79	24.70	−1.13	0.84
Al_2O_3	3.3(1)	3.1(4)	3.3(4)	5(1)	3.2(6)	3.2(3)	3.9(4)	3.63	0.81	0.31	2.88	4.38	4.68	0.57
Fe_2O_3	3.7(3)	4.1(5)	4.0(5)	4(1)	4.0(9)	2.9(4)	3.0(4)	3.61	0.50	0.19	3.15	4.08	−1.36	0.39
SO_3	4.5(1)	4.2(2)	4.3(2)	4.1(5)	5.3(5)	3.9(2)	4.2(2)	4.38	0.44	0.17	3.97	4.78	3.28	0.30
MgO	4.3(1)	3.8(2)	4.1(2)	5.6(4)	4.6(2)	4.2(1)	4.0(2)	4.38	0.61	0.23	3.82	4.94	3.22	0.43
CO_2	3.0(1)	4.0(1)	3.6(1)	3.1(2)	2.7(2)	3.5(1)	3.9(1)	3.40	0.47	0.18	2.96	3.84	−1.44	0.39
H_2O	1.5(1)	1.6(1)	1.6(1)	1.2(1)	1.7(1)	1.6(1)	1.6(1)	1.55	0.15	0.06	1.42	1.69	3.93	0.09
K_2O	1.3(1)	1.0(2)	0.9(2)	0.3(3)	1.2(2)	0.7(1)	0.6(1)	0.86	0.33	0.13	0.56	1.17	−0.42	0.26
Na_2O	0.1(1)	0.0(1)	0.0(1)	0.1(1)	0.03(5)	0.1(1)	0.05(3)	0.04	0.02	0.01	0.03	0.06	−0.29	0.01
Rwp	6.54	13.34	12.33	10.10	12.11	11.62	13.07							
GOF	2.24	2.20	2.03	2.53	2.22	3.71	3.52							

Table 8 – CP III-40RS mass percent composition of main phases and the equivalent oxide composition in columns 1–7 for the diffraction instruments used. Figures are represented with error in brackets affecting the last digit. The columns of the statistical indicators labelled as m for mean, *s* for standard deviation, s_m for standard deviation of mean, l_{95} and u_{95} for lower and upper limits of the 95% confidence intervals of mean, g_2 for the kurtosis parameter and s_a for the mean absolute deviation. The last two rows contain the statistical indicators for the Rietveld refinements.

Phase/Oxide	1	2	3	4	5	6	7	*m*	*s*	s_m	l_{95}	u_{95}	g_2	s_a
Alite (total)	50.7(7)	51(1)	50(1)	51(2)	47.12	52.71	51.35	50.54	1.73	0.65	48.94	52.13	2.92	1.15
Alite (M1)	23.0(7)	21(1)	21(1)	23(2)	18(1)	24(1)	26(1)	22.25	2.67	1.01	19.78	24.72	−0.16	2.10
Alite (M3)	27.7(7)	21(1)	21(1)	23(2)	18(1)	28(1)	25(1)	28.28	1.47	0.56	26.92	29.65	2.27	1.01
Belite	7.1(7)	6.6(7)	7.5(8)	8(2)	11.0(8)	7.5(7)	4.5(7)	7.41	1.91	0.72	5.64	9.18	2.77	1.13
C3A (cub.)	2.8(4)	2.4(4)	2.2(4)	3(1)	2.5(5)	2.7(4)	2.1(4)	2.57	0.37	0.14	2.22	2.91	0.17	0.29
C3A (ort.)	0.6(5)	0.1(5)	0.1(5)	0.0(1)	0.0(1)	0.1(5)	0.2(5)	0.16	0.23	0.09	0.00	0.37	4.49	0.16
Brownmillerite	8.7(6)	8.6(8)	9.6(8)	12(2)	8(1)	8.4(7)	9.5(8)	9.30	1.25	0.47	8.14	10.47	3.93	0.88
Lime	0.0(1)	0.0(1)	0.0(1)	0.3(2)	0.0(1)	0.0(1)	0.0(1)	0.04	0.11	0.04	0.00	0.14	7.00	0.07
Portlandite	0.1(1)	0.2(1)	0.1(1)	0.0(3)	0.7(4)	0.2(2)	0.0(1)	0.19	0.25	0.09	0.00	0.42	4.93	0.16
Periclase	4.2(1)	3.1(2)	3.5(2)	3.6(4)	3.6(2)	3.5(2)	4.1(2)	3.67	0.38	0.14	3.33	4.02	−0.33	0.29
Quartz	0.9(1)	1.2(2)	1.4(2)	0.4(3)	0.3(1)	1.0(1)	1.5(2)	0.97	0.45	0.17	0.55	1.39	−1.09	0.36
Arcanite	2.8(2)	2.7(4)	2.5(4)	2.9(7)	3.0(4)	2.2(3)	2.5(3)	2.66	0.29	0.11	2.40	2.93	0.08	0.23
Langbeinite	4.1(3)	4.5(3)	4.3(3)	1.8(7)	0.6(4)	4.1(3)	4.6(3)	3.43	1.57	0.59	1.97	4.89	0.30	1.28
Aphthitalite	1.7(2)	2.0(3)	1.9(3)	2.0(6)	1.7(3)	1.6(2)	2.0(3)	1.84	0.18	0.07	1.67	2.01	−2.07	0.16
Anhydrite	0.9(1)	1.1(2)	0.9(2)	0.0(3)	1.0(4)	0.9(2)	1.1(2)	0.88	0.40	0.15	0.51	1.25	5.94	0.25
Gypsum	4.3(2)	4.3(3)	4.6(3)	3.0(5)	7.2(5)	3.8(2)	3.9(2)	4.43	1.31	0.49	3.23	5.64	4.16	0.82
Bassanite	1.4(2)	1.3(3)	1.4(3)	2.2(7)	2.8(4)	1.6(2)	1.3(2)	1.73	0.58	0.22	1.19	2.26	1.25	0.46
Calcite	7.9(2)	9.4(4)	8.8(3)	6.5(6)	10.1(4)	8.4(3)	9.8(3)	8.72	1.24	0.47	7.57	9.87	0.51	0.94
Mullite	1.4(3)	1.6(4)	1.3(4)	3.2(9)	0.0(5)	1.2(3)	1.4(3)	1.46	0.93	0.35	0.60	2.31	3.00	0.55
CaO	55.9(4)	55.8(5)	55.6(5)	56(1)	57.3(6)	57.2(4)	55.2(5)	56.21	0.81	0.30	55.47	56.96	−1.33	0.66
SiO_2	17.1(3)	17.3(4)	17.5(4)	17.4(7)	16.5(4)	17.9(3)	16.9(3)	17.25	0.43	0.16	16.85	17.64	0.37	0.32
Al_2O_3	3.1(4)	2.5(4)	2.0(5)	6(1)	2.0(6)	2.5(4)	2.6(4)	2.98	1.41	0.53	1.67	4.28	5.43	0.92
Fe_2O_3	4.1(5)	4.6(6)	5.4(7)	4(1)	3.7(8)	4.2(5)	4.7(6)	4.37	0.57	0.21	3.85	4.90	0.36	0.44
SO_3	7.0(2)	7.2(3)	7.1(3)	5.6(8)	7.9(5)	6.4(3)	7.1(3)	6.91	0.71	0.27	6.26	7.57	1.43	0.50
MgO	4.2(1)	3.1(2)	3.5(2)	3.6(5)	3.5(2)	3.5(2)	4.1(2)	3.67	0.38	0.14	3.33	4.02	−0.33	0.29
CO_2	3.5(1)	4.1(2)	3.9(1)	2.8(4)	4.4(2)	3.7(1)	4.3(1)	3.83	0.55	0.21	3.33	4.34	0.51	0.41
H_2O	1.0(1)	1.0(1)	1.1(1)	0.8(1)	1.8(1)	0.9(1)	0.90(5)	1.08	0.35	0.13	0.76	1.41	5.43	0.22
K_2O	3.8(2)	4.0(2)	3.7(2)	2.9(5)	2.4(3)	3.4(2)	3.9(2)	3.43	0.59	0.22	2.89	3.98	0.34	0.47
Na_2O	0.3(1)	0.4(1)	0.4(1)	0.4(1)	0.3(1)	0.3(1)	0.4(1)	0.36	0.04	0.01	0.33	0.39	−2.07	0.03
Rwp	7.89	12.56	12.25	9.01	8.80	10.85	12.08							
GOF	2.44	2.11	2.06	2.15	2.21	3.53	3.27							

Table 9 – CP IV-32 mass percent composition of main phases and the equivalent oxide composition in columns 1–7 for the diffraction instruments used. Figures are represented with error in brackets affecting the last digit. The columns of the statistical indicators labelled as *m* for mean, *s* for standard deviation, s_m for standard deviation of mean, l_{95} and u_{95} for lower and upper limits of the 95% confidence intervals of mean, g_2 for the kurtosis parameter and s_a for the mean absolute deviation. The last two rows contain the statistical indicators for the Rietveld refinements.

Phase/Oxide	1	2	3	4	5	6	7	*m*	*s*	s_m	l_{95}	u_{95}	g_2	s_a
Alite (total)	43.3(6)	42.1(9)	42.1(9)	39(1)	41.6(9)	43.1(8)	42(1)	41.94	1.50	0.57	40.56	43.32	3.66	0.98
Alite (M1)	18.0(6)	20.4(9)	20.4(9)	19(1)	19.4(9)	19.0(8)	17(1)	19.14	1.10	0.41	18.13	20.15	−0.84	0.82
Alite (M3)	25.3(6)	21.7(9)	21.7(9)	19(1)	22.2(9)	24.1(8)	25(1)	22.80	2.09	0.79	20.86	24.74	−0.99	1.73
Belite	1.9(3)	2.6(5)	2.6(5)	4(1)	3.8(5)	2.9(4)	2.2(5)	2.93	0.93	0.35	2.07	3.79	−0.09	0.72
C3A (cub.)	1.3(4)	0.9(5)	0.9(5)	0.7(5)	1.2(5)	1.5(5)	0.8(5)	1.04	0.29	0.11	0.78	1.31	−1.54	0.25
C3A (ort.)	1.3(4)	0.8(5)	0.8(5)	1.2(6)	0.6(5)	0.7(5)	1.0(5)	0.92	0.26	0.10	0.68	1.16	−1.35	0.22
Brownmillerite	6.9(6)	6.8(7)	6.8(7)	9(1)	6.9(7)	6.1(5)	7.0(7)	7.13	1.09	0.41	6.12	8.14	5.71	0.68
Lime	0.0(1)	0.0(1)	0.0(1)	0.1(1)	0.0(1)	0.0(1)	0.0(1)	0.03	0.06	0.02	0.00	0.09	6.67	0.04
Portlandite	0.8(1)	0.6(1)	0.6(1)	0.2(2)	1.2(2)	0.8(1)	0.6(1)	0.70	0.30	0.11	0.43	0.98	1.86	0.20
Periclase	4.7(1)	4.9(2)	4.9(2)	5.3(3)	4.0(2)	4.9(2)	3.8(2)	4.64	0.53	0.20	4.15	5.12	−0.63	0.41
Quartz	14.2(2)	13.9(3)	13.9(3)	13.6(5)	13.8(4)	13.6(3)	14.6(4)	13.93	0.36	0.14	13.60	14.26	1.28	0.26
Arcanite	0.9(2)	1.0(3)	1.0(3)	1.0(3)	1.1(3)	0.6(2)	0.7(2)	0.93	0.17	0.07	0.77	1.09	−0.32	0.14
Langbeinite	0.1(1)	0.4(2)	0.3(2)	0.0(4)	0.0(4)	0.2(2)	0.9(2)	0.28	0.32	0.12	0.00	0.57	2.67	0.23
Aphthitalite	0.8(1)	1.0(2)	1.1(2)	0.3(2)	0.7(2)	0.9(1)	1.1(2)	0.87	0.26	0.10	0.63	1.11	1.82	0.19
Anhydrite	0.6(1)	0.9(2)	0.9(2)	0.0(2)	0.9(3)	0.7(1)	0.9(2)	0.71	0.33	0.12	0.41	1.01	3.51	0.23
Gypsum	4.5(1)	4.3(2)	4.3(2)	2.9(3)	3.1(4)	4.5(2)	4.7(2)	4.06	0.71	0.27	3.40	4.72	−0.76	0.58
Bassanite	0.6(1)	0.6(2)	0.6(2)	2.2(4)	1.6(3)	0.9(1)	0.6(2)	1.02	0.63	0.24	0.44	1.60	0.98	0.50
Calcite	5.1(2)	5.3(2)	5.3(2)	4.8(4)	5.3(3)	5.6(2)	6.1(3)	5.37	0.40	0.15	5.00	5.74	0.92	0.27
Mullite	12.9(3)	13.8(5)	13.8(5)	14.6(7)	14.1(5)	12.9(4)	12.4(4)	13.50	0.80	0.30	12.76	14.24	−1.16	0.66
CaO	43.3(4)	42.2(6)	42.2(6)	42.0(9)	43.3(6)	43.6(5)	43.2(6)	42.83	0.68	0.26	42.21	43.46	−2.38	0.61
SiO_2	29.7(3)	29.6(4)	29.6(4)	29.3(6)	29.9(4)	29.4(3)	29.9(4)	29.65	0.22	0.08	29.44	29.85	−1.34	0.18
Al_2O_3	11.2(3)	11.0(5)	11.0(4)	13.5(8)	12.4(5)	10.8(4)	10.4(5)	11.47	1.04	0.39	10.51	12.44	0.81	0.81
Fe_2O_3	3.0(4)	3.5(5)	3.5(5)	3(1)	2.3(6)	2.9(4)	3.3(5)	3.08	0.44	0.17	2.68	3.49	1.46	0.32
SO_3	3.7(2)	4.0(2)	4.0(2)	3.3(4)	3.8(4)	3.8(2)	4.3(2)	3.84	0.33	0.12	3.54	4.14	0.79	0.24
MgO	4.7(1)	4.9(2)	4.9(2)	5.3(3)	4.0(2)	4.9(2)	3.8(2)	4.64	0.53	0.20	4.15	5.12	−0.63	0.41
CO_2	2.2(1)	2.3(1)	2.3(1)	2.1(2)	2.3(1)	2.5(1)	2.7(1)	2.36	0.18	0.07	2.20	2.52	0.92	0.12
H_2O	1.2(1)	1.1(1)	1.1(1)	0.8(1)	1.0(1)	1.2(1)	1.2(1)	1.08	0.14	0.05	0.96	1.21	3.80	0.09
K_2O	0.8(1)	1.0(2)	1.0(2)	0.7(3)	0.8(2)	0.7(1)	1.1(2)	0.88	0.18	0.07	0.71	1.04	−2.01	0.15
Na_2O	0.2(1)	0.2(0)	0.2(1)	0.1(1)	0.15(4)	0.2(1)	0.21(3)	0.17	0.05	0.02	0.12	0.22	1.82	0.04
Rwp	5.78	10.71	10.71	5.67	8.60	9.22	11.34							
GOF	2.06	1.97	1.97	1.57	1.67	3.25	3.32							

Table 10 – CP V-ARI mass percent composition of main phases and the equivalent oxide composition in columns 1–7 for the diffraction instruments used. Figures are represented with error in brackets affecting the last digit. The columns of the statistical indicators labelled as *m* for mean, *s* for standard deviation, s_m for standard deviation of mean, l_{95} and u_{95} for lower and upper limits of the 95% confidence intervals of mean, g_2 for the kurtosis parameter and s_a for the mean absolute deviation. The last two rows contain the statistical indicators for the Rietveld refinements.

Phase/Oxide	1	2	3	4	5	6	7	*m*	*s*	s_m	l_{95}	u_{95}	g_2	s_a	
Alite (total)	59.2(4)	58.8(7)	58.8(7)	55.5(9)	59.1(9)	60.2(6)	59.7(7)	58.78	1.49	0.56	57.40	60.16	4.86	0.91	
Alite (M1)	31.7(4)	34.1(7)	33.0(7)	29(1)	29.5(9)	27.8(6)	31.2(7)	30.93	2.22	0.84	28.88	32.99	−1.00	1.78	
Alite (M3)	27.6(4)	24.7(7)	25.8(7)	26(1)	29.6(9)	32.4(6)	28.5(7)	27.85	2.60	0.98	25.45	30.25	0.28	1.98	
Belite	10.2(3)	10.3(5)	10.2(4)	12(1)	8.2(5)	10.9(3)	10.2(4)	10.27	1.09	0.41	9.26	11.27	2.75	0.64	
C3A (cub.)	4.6(2)	4.4(3)	4.4(3)	4.0(7)	4.0(6)	4.7(2)	4.0(3)	4.31	0.30	0.11	4.03	4.59	−1.64	0.25	
C3A (ort.)	0.2(2)	0.4(3)	0.3(3)	0.5(6)	0.8(6)	0.0(3)	0.2(3)	0.35	0.24	0.09	0.13	0.58	0.87	0.18	
Brownmillerite	9.1(3)	8.9(4)	8.7(4)	12(1)	9.8(6)	8.5(3)	9.1(4)	9.39	1.04	0.39	8.44	10.35	3.97	0.73	
Lime	0.1(1)	0.0(1)	0.1(1)	0.5(2)	0.1(1)	0.0(1)	0.2(1)	0.15	0.17	0.06	0.00	0.31	4.96	0.11	
Portlandite	1.1(1)	0.9(1)	0.8(1)	0.6(4)	0.8(2)	1.4(1)	0.7(1)	0.91	0.28	0.10	0.66	1.17	1.47	0.20	
Periclase	5.8(1)	6.2(1)	6.2(1)	7.1(3)	6.2(2)	6.5(1)	7.0(1)	6.45	0.46	0.17	6.02	6.87	−0.93	0.36	
Quartz		0.3(1)	0.3(1)	0.4(1)	0.2(2)	0.2(1)	0.4(1)	0.3(1)	0.31	0.08	0.03	0.24	0.39	−1.03	0.07
Arcanite	0.6(1)	0.6(2)	0.6(2)	0.0(3)	0.2(3)	0.2(1)	0.1(1)	0.32	0.28	0.11	0.06	0.58	−2.38	0.25	
Langbeinite	0.7(1)	0.6(2)	0.7(1)	0.0(4)	0.3(2)	0.3(1)	0.8(1)	0.51	0.30	0.11	0.23	0.78	−0.55	0.25	
Aphthitalite	0.6(1)	0.4(1)	0.3(1)	0.1(2)	0.1(2)	0.4(1)	0.5(1)	0.35	0.19	0.07	0.17	0.53	−0.35	0.14	
Anhydrite	0.1(1)	0.1(1)	0.2(1)	0.0(2)	1.2(4)	0.1(1)	0.3(1)	0.29	0.40	0.15	0.08	0.66	5.92	0.25	
Gypsum	1.1(1)	1.4(1)	1.6(1)	1.1(2)	2.4(4)	1.4(1)	1.5(1)	1.51	0.44	0.17	1.10	1.92	3.41	0.29	
Bassanite	2.7(1)	2.5(2)	2.4(2)	2.8(5)	3.4(3)	2.6(1)	2.3(1)	2.70	0.37	0.14	2.35	3.04	3.03	0.26	
Calcite	2.5(1)	3.2(2)	3.2(2)	2.7(3)	2.9(2)	2.0(1)	2.6(2)	2.73	0.44	0.17	2.32	3.14	0.09	0.34	
Mullite	0.9(2)	0.6(2)	0.8(2)	1.3(5)	0.1(2)	0.3(1)	0.4(2)	0.66	0.41	0.15	0.28	1.03	0.09	0.31	
CaO	61.2(2)	61.2(3)	61.0(3)	60.8(6)	61.6(4)	62.1(2)	61.2(2)	61.29	0.41	0.16	60.91	61.67	1.45	0.30	
SiO_2	19.7(1)	19.5(2)	19.7(2)	19.3(5)	18.7(3)	20.1(1)	19.7(2)	19.54	0.45	0.17	19.13	19.95	2.07	0.31	
Al_2O_3	3.5(2)	3.3(3)	3.4(3)	5.3(7)	4.3(4)	3.4(2)	3.1(2)	3.77	0.79	0.30	3.04	4.50	2.16	0.60	
Fe_2O_3	4.0(2)	4.0(3)	3.8(3)	4(1)	2.8(4)	3.3(2)	3.9(3)	3.63	0.47	0.18	3.20	4.06	0.91	0.37	
SO_3	2.9(1)	2.8(2)	2.9(2)	2.1(4)	4.0(4)	2.5(1)	2.7(1)	2.87	0.56	0.21	2.35	3.39	2.93	0.35	
MgO	5.8(1)	6.2(1)	6.2(1)	7.1(3)	6.2(2)	6.5(1)	7.0(1)	6.45	0.46	0.17	6.02	6.87	−0.93	0.36	
CO_2	1.1(1)	1.4(1)	1.4(1)	1.2(1)	1.3(1)	0.9(1)	1.1(7)	1.20	0.20	0.07	1.02	1.38	0.09	0.15	
H_2O	0.7(1)	0.7(1)	0.7(1)	0.5(1)	0.9(1)	0.8(1)	0.64(3)	0.71	0.12	0.04	0.60	0.81	0.86	0.09	
K_2O	0.8(1)	0.7(1)	0.8(1)	0.1(2)	0.3(2)	0.3(1)	0.50(1)	0.49	0.29	0.11	0.22	0.76	−1.09	0.24	
Na_2O	0.1(1)	0.1(1)	0.1(1)	0.1(1)	0.02(3)	0.1(1)	0.09(2)	0.07	0.04	0.01	0.03	0.10	−0.35	0.03	
Rwp	5.24	10.57	10.28	9.50	8.70	8.10	9.80								
GOF	1.66	1.73	1.69	2.33	1.50	2.53	2.57								

Conclusions

This is the first time that the possibility of determining the M1 and M3 polymorphs of alite in cementitious materials by X-ray powder diffraction has been studied in a fairly systematic way by means of testing instruments from different laboratories. Likewise, the capacities of several Brazilian powder diffraction laboratories to carry out mineralogical analyses of Portland-type cementitious materials were tested.

The results seem to be promising because by optimising the sample preparation procedures and the data collection strategy, it will be possible to have one more analytical technique for the quality control of Portland cement products.

Although powder diffraction allows the quantitative determination of the main crystalline phases, such as polymorphs of alite, belite, cubic and orthorhombic tricalcium aluminate, brownmillerite, mullite, calcium carbonate and gypsum, it has become clear that it is a complementary method to that of X-rays. fluorescence. This last technique is irreplaceable for evaluating minor species containing sulphur, magnesium, sodium or potassium.

The next logical step would be to extend the study to more complex cement samples, including the evaluation of the non-crystalline fraction, and invite laboratories to participate in this exercise using other models for the quantification of M1 and M3 with different Rietveld packages and following more precise protocols in line with the guidelines of the publications cited here, with the ultimate goal of establishing new technical standards for the quality control of cements.

Acknowledgments

C.M. Rossetto would like to thank Centro Paula Souza – CPS for having approved her research Project. X. Turrillas, would like to acknowledge the financial support from the MINECO Project no. BIA2014-57658-C2-1-R, Jan 1st 2015 to Dec 31st 2017 and also to acknowledge the MINECO award "Centro de Excelencia Severo Ochoa" FUNFUTURE (CEX2019-000917-S) granted to ICMAB.

The authors would like to thank ABCP-Brazilian Association of Portland Cement for kindly supplying the samples and the corresponding chemical analyses.

Alicia Manjón of MSPD beamline is acknowledged for the acquisition of synchrotron diffraction pattern.

Anna Crespi, Joan B. Esquius, Francesc Xavier Campos and Jordi Rius of ICAMB X-ray Laboratory are acknowledged for the X-ray diffraction data acquisition.

REFERENCES

[1] H.M. Rietveld, A profile refinement method for nuclear and magnetic structures, J. Appl. Crystallogr. 2 (1969) 65–71, http://dx.doi.org/10.1107/S0021889869006558.

[2] N.V.Y. Scarlett, I.C. Madsen, C. Manias, D. Retallack, On-line X-ray diffraction for quantitative phase analysis: application in the Portland cement industry, Powder Diff. 16 (2) (2001) 71–80, http://dx.doi.org/10.1154/1.1359796.

[3] O. Pritula, L. Smrcok, On reproducibility of Rietveld analysis of reference Portland cement clinkers, Powder Diff. 18 (1) (2003) 16–22, http://dx.doi.org/10.1154/1.1545116.

[4] P. Stutzman, Powder diffraction analysis of hydraulic cements: ASTM Rietveld round-robin results on precision, Powder Diff. 20 (2) (2005) 97–100, http://dx.doi.org/10.1154/1.1913712.

[5] L. León-Reina, A.G. De la Torre, J.M. Porras-Vázquez, M. Cruz, L.M. Ordonez, X. Alcobé, F. Gispert-Guirado, A. Larranaga-Varga, M. Paul, T. Fuellmann, R. Schmidt, M.A.G. Aranda, Round robin on Rietveld quantitative phase analysis of Portland cements, J. Appl. Crystallogr. 42 (2009) 906–916, http://dx.doi.org/10.1107/S0021889809028374.

[6] M.A.G. Aranda, A.G. De la Torre, L. León-Reina, Rietveld quantitative phase analysis of OPC clinkers, cements and hydration products, Rev. Mineral. Geochem. 74 (2012) 169–209, http://dx.doi.org/10.2138/rmg.2012.74.5.

[7] P. Stutzman, Quantitative X-ray powder diffraction analysis of portland cements: proficiency testing for laboratory assessment, ASTM Int. Adv. Civ. Eng. Mater. 3 (1) (2014), http://dx.doi.org/10.1520/ACEM20130093.

[8] R. Snellings, in: K. Scrivener, R. Snellings, B. Lothenbach (Eds.), X-ray Powder Diffraction Applied to Cement, A Practical Guide to Microstructural Analysis of Cementitious Materials, 1st edition, CRC Press, 2016, ISBN 9781351228497, http://dx.doi.org/10.1201/b19074.

[9] A.F. Gualtieri, G.D. Gatta, R. Arletti, G. Artioli, P. Ballirano, G. Cruciani, A. Guagliardi, D. Malferrari, N. Masciocchi, P. Scardi, Quantitative phase analysis using the Rietveld method: towards a procedure for checking the reliability and quality of the results, Period. Mineral. 88 (2019) 147–151, http://dx.doi.org/10.2451/2019PM870.

[10] M.A.G. Aranda, A.G. De la Torre, L. Leon-Reina, in: C.J. Gilmore, J.A. Kaduk, H. Schenk (Eds.), International Tables for Crystallography Volume H: Powder-diffraction, 2019, ISBN 978-1-118-41628-0, p. 855, http://dx.doi.org/10.1107/97809553602060000115.

[11] M.R. Rowles, The effect of data quality and model parameters on the quantitative phase analysis of X-ray diffraction data by the Rietveld method, J. Appl. Crystallogr. 54 (2021) 878–894, http://dx.doi.org/10.1107/S160057672100371X.

[12] H.F.W. Taylor, Cement Chemistry, Tomas Telford Publishing, London E144JD, 1997, https://www.icevirtuallibrary.com/doi/pdf/10.1680/cc.25929.fm.

[13] T. Staněk, P. Sulovský, The impact of basic minor oxides on the clinker, Mater. Sci. For. 908 (2017) 3–9, http://dx.doi.org/10.4028/www.scientific.net/MSF.908.3.

[14] H.-M. Ludwig, W. Zhang, Research review of cement clinker chemistry, Cem. Concr. Res. 78 (2015) 24–37, http://dx.doi.org/10.1016/j.cemconres.2015.05.018.

[15] A.G. De la Torre, R.N. de Vera, A.J.M. Cuberos, M.A.G. Aranda, Crystal structure of low-magnesium content alite: application to Rietveld quantitative phase analysis, Cem. Concr. Res. 38 (11) (2008) 1261–1269, http://dx.doi.org/10.1016/j.cemconres.2008.06.005.

[16] A.G. De la Torre, E.R. Losilla, A. Cabeza, M.A.G. Aranda, High-resolution synchrotron powder diffraction analysis of ordinary Portland cements: Phase coexistence of alite, Nucl. Instr. Methods Phys. Res. Sect. B: Beam Int. Mater. Atoms 238 (1–4) (2005) 87–91, http://dx.doi.org/10.1016/j.nimb.2005.06.023.

[17] A.G. De la Torre, S. Bruque, J. Campo, M.A.G. Aranda, The superstructure of C3S from synchrotron and neutron powder

diffraction and its role in quantitative phase analyses, Cem. Concr. Res. 32 (2002) 1347–1356, http://dx.doi.org/10.1016/j.nimb.2005.06.023.
[18] F. Dunstetter, M.N. De Noirfontaine, M. Courtial, Polymorphism of tricalcium silicate, the major compound of Portland cement clinker: 1. Structural data: review and unified analysis, Cem. Concr. Res. 36 (1) (2006) 39–53, http://dx.doi.org/10.1016/j.cemconres.2004.12.003.
[19] M.-N. de Noirfontaine, M. Courtial, F. Dunstetter, G. Gasecki, M. Signes-Frehel, Tricalcium silicate Ca_3SiO_5 superstructure analysis: a route towards the structure of the M1 polymorph, Zeitschr. Kristallogr. Gruyt. 227 (2012) 102–112, http://dx.doi.org/10.1524/zkri.2012.1425.
[20] T. Staněk, P. Sulovský, The influence of the alite polymorphism on the strength of the Portland cement, Cem. Concr. Res. 32 (7) (2002) 1169–1175, http://dx.doi.org/10.1016/S0008-8846(02)00756-1.
[21] A.A. Coelho, TOPAS and TOPAS-Academic: an optimization program integrating computer algebra and crystallographic objects written in C++, J. Appl. Crystallogr. 51 (1) (2018) 210–218, http://dx.doi.org/10.1107/S1600576718000183.
[22] G.S. Pawley, Unit-cell refinement from powder diffraction scans, J. Appl. Crystallogr. 14 (1981) 357–361, http://dx.doi.org/10.1107/S0021889881009618.
[23] J.F. Natalli, E.C.S. Thomaz, J.C. Mendes, R.A.F. Peixoto, A review on the evolution of Portland cement and chemical admixtures in Brazil, Rev. IBRACON Estrut. Mater. 14 (6) (2021), http://dx.doi.org/10.1590/S1983-41952021000600003, e14603.
[24] J.C. Zwinkels, P.C. DeRose, J.E. Leland, Spectral fluorescence measurements, in: T.A. Germer, J.C. Zwinkels, B.K. Tsai (Eds.), Experimental Methods in the Physical Sciences, Vol. 46, Academic Press, 2014, pp. 221–290 (Chapter 7). ISSN 1079-4042, ISBN 9780123860224.
[25] Origin V.8 (2007) Windows, OriginLab Corporation, Northampton, MA, USA, 2007, https://www.originlab.com/pdfs/origin_8.1_getting_started_booklet.pdf.
[26] G.V. Hartland, Statistical analysis of physical chemistry data: errors are not mistakes, J. Phys. Chem. A 124 (2020) 2109–2112, http://dx.doi.org/10.1021/acs.jpca.0c01403.
[27] L.B. McCusker, R.B. Von Dreele, D.E. Cox, D. Louer, P. Scardi, Rietveld refinement guidelines, J. Appl. Crystallogr. 32 (Pt. 1) (1999) 36–50, https://onlinelibrary.wiley.com/iucr/doi/10.1107/S0021889898009856.
[28] W.A. Dollase, Correction of intensities for preferred orientation in powder diffractometry: application of the March model, J. Appl. Crystallogr. 19 (4) (1986) 267–272, http://dx.doi.org/10.1107/S0021889886089458.
[29] F. Nishi, Y. Takeuchi, I. Maki, The tricalcium silicate $Ca_3O[SiO_4]$: the monoclinic superstructure, Z. Kristallogr. 172 (1985) 297–314, http://dx.doi.org/10.1524/zkri.1985.172.14.297.
[30] W.G. Mumme, R.J. Hill, G. Bushnell-Wye, E.R. Segnit, Rietveld crystal structure refinement, crystal chemistry and calculated powder diffraction data for the polymorphs of dicalcium silicate and related phases, Neu. Jahrb. Mineral. Abhandlungen 169 (1995) 35–68, http://hdl.handle.net/102.100.100/234637?index=1.
[31] P. Mondal, J.W. Jeffery, The crystal structure of tricalcium aluminate $Ca_3Al_2O_6$, Acta Crystallogr. 31 (3) (1975) 689–697, http://dx.doi.org/10.1107/S0567740875003639.
[32] A.A. Colville, S. Geller, The crystal structure of brownmillerite, Ca_2FeAlO_5, Acta Crystallogr. Sect. B: Struct. Sci. Cryst. Eng. Mater. B27 (1971) 2311–2315, http://dx.doi.org/10.1107/S056774087100579X.
[33] F. Nishi, Y. Takeuchi, The Al_6O_{18} rings of tetrahedra un the structure of $Ca_8.5NaAl_6O_{18}$, Acta Crystallogr. Sect. B: Struct. Sci. Cryst. Eng. Mater. 31 (1975) 1169–1173, http://dx.doi.org/10.1107/S0567740875004736.
[34] D.L. Graf, Crystallographic tables for the rhombohedral carbonates, Am. Mineral. 46 (11–12) (1961) 1283–1316.
[35] D.M. Henderson, H.S. Gutowsky, A nuclear magnetic resonance determination of the hydrogen positions in $Ca(OH)_2$, Am. Mineral. 47 (11–12) (1962) 1231–1251.
[36] R.M. Hazen, Effects of temperature and pressure on the cell dimension and X-ray temperature, factors of periclase, Am. Mineral. 61 (1976) 266–271, http://citeseerx.ist.psu.edu/viewdoc/download?doi=10.1.1.558.5675&rep=rep1&type=pdf (03/02/2022).
[37] R.J. Angel, C.T. Prewitt, Crystal structure of mullite: a re-examination of the average structure, Am. Mineral. 71 (11–12) (1986) 1476–1482.
[38] J.A. McGinnety, Redetermination of the structures of potassium sulphate and potassium chromate: the effect of electrostatic crystal forces upon observed bond length, Acta Crystallogr. Sect. B 28 (1972) 2845–2852, http://dx.doi.org/10.1107/S0567740872007022.
[39] D. Speer, E. Salje, Phase transitions in langbeinites I: Crystal chemistry, and structures of K-double sulfates of the langbeinite type $M_2^{++}K_2(SO_4)_3$, M^{++} = Mg, Ni, Co, Zn, Ca, Phys. Chem. Miner. 13 (1986) 17–24, http://dx.doi.org/10.1007/BF00307309.
[40] F.C. Hawthorne, R.B. Ferguson, Anhydrous sulphates. II. Refinement of the crystal structure of anhydrite, Can. Mineral. 13 (1975) 289–292.
[41] P. Ballirano, A. Maras, S. Meloni, R. Caminiti, The monoclinic I2 structure of bassanite, calcium sulphate hemihydrate ($CaSO{\cdot}0.5H_2O$), Eur. J. Mineral. 13 (2001) 985–993, http://dx.doi.org/10.1127/0935-1221/2001/0013-0985.
[42] P.F. Schofield, K.S. Knight, I.C. Stretton, Thermal expansion of gypsum investigated by neutron powder diffraction, Am. Mineral. 81 (1996) 847–851, http://dx.doi.org/10.2138/am-1996-7-807.
[43] K. Okada, J. Ossaka, Structures of potassium sodium sulphate and tripotassium sodium disulphate, Acta Crystallogr. Sect. B36 (1980) 919–921, http://dx.doi.org/10.1107/S0567740880004852.
[44] R.E. Dinnebier, J.S.O. Evans, A. Leineweber, Rietveld Refinement: Practical Powder Diffraction Pattern Analysis Using TOPAS, De Gruyter STEM, Berlin, Germany, 2019, ISBN 9783110456219.
[45] I.C. Madsen, N.V.Y. Scarlett, A. Kern, Description and survey of methodologies for the determination of amorphous content via X-ray powder diffraction, Z. Kristallogr. 226 (2011) 944–955, http://dx.doi.org/10.1524/zkri.2011.1437.
[46] A.F. Gualtieri, V. Riva, A. Bresciani, S. Maretti, M. Tamburini, A. Vianic, Accuracy in quantitative phase analysis of mixtures with large amorphous contents. The case of stoneware ceramics and bricks, J. Appl. Cryst. 47 (3) (2014) 835–846, http://dx.doi.org/10.1107/S160057671400627X.
[47] P.M. Suherman, A. van Riessen, B. O'Connor, D. Li, D. Bolton, H. Fairhurst, Determination of amorphous phase levels in Portland cement clinker, Powder Diff. 17 (3) (2002) 178–185, http://dx.doi.org/10.1154/1.1471518.
[48] P.E. Stutzman, G. Lespinasse, S. Leigh, Compositional analysis and certification of NIST reference material clinker 2686a, 30th International Conference on Cement Microscopy, AT: Reno, 2008, ResearchGate. https://www.researchgate.net/publication/258870551_Compositional_Analysis_and_Certification_of_NIST_Reference_Material_Clinker_2686a.